Eur. Phys. J. Special Topics **213**, 355–365 (2012)

DOI: 10.1140/epjst/e2012-01682-3

THE EUROPEAN PHYSICAL JOURNAL SPECIAL TOPICS

Regular Article

Diffraction studies on natural and model lipid bilayers

F. Sebastiani[1,2], R. Harvey[3,a], S. Khanniche[1,b], J.-B. Artero[1,4], M. Haertlein[1], and G. Fragneto[1]

[1] Institut Laue Langevin, 6 rue Jules Horowitz, BP. 156, 38042 Grenoble, France
[2] Dipartimento di Fisica, Università di Roma "Tor Vergata", via della Ricerca Scientifica 1, 00133 Roma, Italy
[3] Institute of Pharmaceutical Science, King's College London, Franklin-Wilkins Building, 150 Stamford Street, London SE1 9NH, UK
[4] Macromolecular Structure Research Group, Keele University, Keele, Staffordshire, UK

Received 20 July 2012 / Received in final form 27 September 2012
Published online 3 December 2012

Abstract. In this study we have used neutron diffraction to examine the swelling behaviour and bilayer parameters of membranes reconstituted from polar lipids extracted from *B. subtilis* and model systems composed of synthetic phospholipids. Evidence for phase separation in the model system (lacking in Lysyl-PG, L-PG) is discussed in relation to its possible contribution to membrane domain formation through lipid-lipid interactions. Comparing these results with those obtained from the bilayers composed of lipids extracted from bacterial cells gives us some indication of the role of L-PG in the *B. subtilis* plasma membrane.

1 Introduction

The common soil bacterium *Bacillus subtilis* has attained a similar status to that of Gram negative *Escherichia coli*, in that its biochemistry, physiology and genetics have been extensively studied and characterised to the extent that it is considered a model for many other Gram positive organisms. [1] One aspect of bacterial physiology which has recently gained in prominence is what could be termed the functional lipidomics of their plasma membranes; how the plasticity of lipid composition ensures the maintenance of membrane function despite exposure to fluctuating environmental conditions. [1,2] In Gram positive bacteria such as *B. subtilis*, the lipid component of the plasma membrane is not only the sole permeability barrier of the cell, but it also provides a matrix or attachment point for a variety of functional and structural proteins as well as taking an active role in cell growth, reproduction and defence against certain antibiotics. [3,4] These varied roles of plasma membrane lipids are thought to be facilitated by the presence of discrete domains, functional zones of characteristic lipid composition, the formation of which may be driven both by specific lipid-lipid and lipid-protein interactions. [5] With respect to lipid-lipid interactions

[a] e-mail: richard.d.harvey@kcl.ac.uk
[b] *Current affiliation*: CEA, DAM, Le Ripault, 37260 Monts, France

alone, in *B. subtilis*, it is the physical properties of its four major phospholipids; anionic phosphatidylglycerol (PG) and cardiolipin (CL), zwitterionic phosphatidylethanolamine (PE) and cationic lysyl-phosphatidylglycerol (L-PG), which are thought to be responsible for facilitating both domain formation and antibiotic resistance, [3,6] making the study of the interactions between these lipids crucial to our understanding of the physiology of Gram positive bacteria.

The distribution of PG, PE, CL and L-PG in the plasma membrane of *B. subtilis* has been shown to be localised into regions rich in one or more of each phospholipid type. [7] Regions which exhibit high degrees of membrane curvature such as the poles of the cell and the septum which forms during cell division are rich in CL and PE, whilst the long axes of these rod-shaped cells possess helical PG-rich domains. [8] L-PG is closely associated with PG, as the relative proportions of these lipids are regulated in response to various environmental stimuli such as fluctuations in pH and the presence of natural antibiotic substances. [6,9] The packing geometries of both CL and PE are known to favour the formation of curved bilayers, [10,11] which would explain their localisation in regions of the membrane where a high degree of curvature is either permanent or transient. The apparent phase separation between PG and PE which results in the helical PG domain appears to arise from a combination of protein-lipid interactions and the effect of environmental conditions upon the intrinsic properties of the lipids. Demixing of PG and PE has been shown to occur more readily in *B. subtilis* membranes than in liposomes containing synthetic lipids, with PE lipids being recruited into proteo-lipid domains. [5] PG itself may associate with cytoskeletal proteins which are organised into spirals adjacent to the cell membrane, but it is unclear as to whether the lipid domains form as a result of presence of the protein, or *vice versa*. [7]

There is, however, some evidence that demixing can occur between PE and PG which is driven by lipid-lipid interactions alone. X-ray diffraction studies on POPE/POPG mixtures at pH 7.4 show a transition from a single phase to two separate phases when the proportion of PG increases above 0.7. [12] Theoretically, in the mildly acidic conditions encountered at the plasma membrane of *B. subtilis* during active growth, some protonation of the PG would occur which could further encourage demixing from PE due to their differing headgroup properties. [13] The influence of L-PG on the phase behaviour of such lipid mixtures remains unexamined, largely due to the highly labile nature of the L-PG headgroup making its characterisation using diffraction techniques prone to artefacts. [14] It has been speculated, however, that the cationic nature of L-PG and its putative propensity to form ion pairs with PG or CL would serve to dampen the overall anionic charge on the *B. subtilis* membrane. [9] Since the addition of even a small proportion of POPG ($\sim$0.1) produces a dramatic increase in lamellar repeat spacing (from $\sim$62 Å to $\sim$113 Å) in POPE bilayers under the influence of Coulombic forces, [12] any significant charge dampening by L-PG may be detected by the formation of phases with intermediate lamellar periodicity.

In this study we have used neutron diffraction to examine the swelling behaviour and bilayer parameters of membranes reconstituted from polar lipids extracted from *B. subtilis* and model systems composed of synthetic phospholipids. Evidence for phase separation in the model system (lacking in L-PG) is discussed in relation to its possible contribution to membrane domain formation through lipid-lipid interactions.

2 Materials and methods

2.1 Extraction of *Bacillus subtilis* membrane lipids

Bacillus subtilis (ATCC 6051) was cultured for 34 hours at 37 °C in 1.5 L of minimal medium $(2.5\,\mathrm{g/L}\,(NH_4)_2SO_4, 1\mathrm{g/L}\,(NH_4)_2-\mathrm{H}-\mathrm{citrate}, \quad 0.25\,\mathrm{g/L}\,MgSO_4, \quad 10\,\mathrm{g/L}$

glycerol, 5g/L K_2HPO_4/KH_2PO_4, 0.1 g/L $CaCl_2$, 0.1 g/L $MnSO_4$, 0.1 g/L $FeSO_4$, 0.2 g/L $ZnSO_4$) adjusted to pH 7 with phosphate buffer, in a Labfors 2 (Infors-HT, Switzerland) batch fermentation unit under constant aeration. The cells were harvested by centrifugation at 6000 rpm for 20 minutes at 4 °C (Beckman High-Speed centrifuge). The polar lipids were isolated from cell paste by following the chloroform-methanol-water extraction method of Bligh and Dyer. [15] Lipid extract purity was monitored by thin layer chromatography using a chloroform-methanol-acetic acid-water (250 : 74 : 19 : 3, v/v/v/v) mobile phase, with the relative proportions of each of the major constituent phospholipids found to be comparable with those previously reported for *B. subtilis* ATCC 6051 grown under similar conditions (∼12% CL, ∼30% PE, ∼36% PG and ∼22% L-PG.). [16]

2.2 Sample preparation

The substrates used to support the samples were 5 cm diameter silicon wafers, with a thickness of 0.5 mm. Surfaces were first treated with a Piranha solution [17]. Highly hydrophilic surfaces were obtained by solvent treatment sonication of each wafer in different solvents (chloroform, acetone and ethanol) followed by a UV/ozone treatment for 30 minutes [18]. Ellipsometry measurements indicated that the oxide layer thickness of the wafers was similar for all samples and around 1 nm.

The lipid extract was dissolved in Trifluoroethanol/Chloroform (1 : 1) (Sigma-Aldrich) at a concentration of 35 mg/ml. The deposition was made by spin coating, choosing a unique step (5000 rpm for 30 s).

Other samples were prepared with synthetic phospholipids to mimic the phospholipid composition of *Bacillus subtilis* [19]: a neutral sample prepared from pure 1-palmitoyl-2-oleoyl-*sn*-glycero-3-phosphoethanolamine (POPE); a charged sample prepared from pure 1-palmitoyl-2-oleoyl-*sn*-glycero -3-phospho-(1'-*rac*-glycerol) (sodium salt) (POPG); and a mixed sample consisting of 40% POPE, 20% POPG and 40% Cardiolipin (CL). Lysyl-DPPG (1,2-dipalmitoyl-sn-glycero-3-[phospho-rac-(3-lysyl(1-glycerol))]) was not used because problems were encountered while dissolving the compound.

POPE (>99% purity), POPG (>99% purity) and Cardiolipin (>99% purity) were purchased from Avanti Polar Lipids (Alabaster, AL) and used without further purification. A mixture of Chloroform/Methanol (2 : 1) was used to dissolve the phospholipids; both solvents were purchased from Sigma-Aldrich. The volume of solutions used was 0.9 ml, with a molar concentration of $1.208 \cdot 10^{-5}$ mole/ml. All samples were prepared by spin coating, following four stages of increasing rotation speed, each 30 s long (100 rpm, 200 rpm, 500 rpm and 800 rpm).

In order to remove solvent residues, samples were kept under vacuum for several hours. Samples were then hydrated in a high relative humidity cell for at least 48 hours. High relative humidity was obtained by introducing a saturated aqueous solution of anhydrous sodium sulphate inside a sealed cell in an oven at 50 °C. This procedure is known as annealing. After annealing, samples must show a thickness increase from dried conditions and that was confirmed by ellipsometry measurements. Microscopically, moving from dried to hydrated conditions, samples increase their thickness because water molecules are present in the spaces between adjacent bilayers. Before the experiment, the samples were kept in a saturated D_2O vapour for at least 24 hours.

2.3 Experimental setup

It was experimentally demonstrated by John Katsaras [20] that the bilayer behaviour is the same in 100% relative humidity and in bulk water. A multi-layered sample

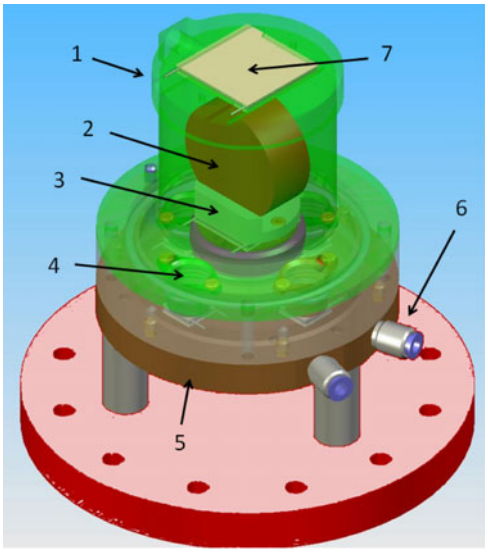

Fig. 1. Schematics of the humidity chamber. (1) Aluminum cover, (2) sample, (3) sample holder, (4) one of the four water reservoirs in aluminum on the basis of the chamber, (5) water cooler, (6) thermal bath connectors for the water cooler, (7) Peltier element for the cover.

is usually not stable in bulk solvent, therefore measurements were performed in a humidity controlled environment. The humidity chamber used in this study allows the simultaneous control of temperature and humidity, retaining sample stability during long data acquisitions [21]. Theoretically, the relative humidity at a given temperature may be calculated with the Equation [22]:

$$\mathrm{RH}(\%) = \frac{\mathrm{P}(\mathrm{T_w})}{\mathrm{P}(\mathrm{T_s})} \cdot 100 \tag{1}$$

where RH is the relative humidity in percent in air or in another gas. P(T) is the partial pressure of water at a given temperature; $\mathrm{T_w}$ is the temperature of the water reservoir and $\mathrm{T_s}$ the temperature of the sample. A common way to vary the humidity content of a sample is to put it in contact with vapour from saturated salt solutions. The disadvantage of this method is that humidity cannot be varied continuously. At the ILL a humidity chamber, that allows continuous change in RH, was built and then upgraded for this work. The chamber has a temperature control for water reservoirs, sample holder and cover; furthermore humidity and temperature sensors are located close to the sample. By varying independently the temperature of the two compartments of the chamber (water reservoir and top part containing the sample) it is possible to vary continuously the humidity according to Equation (1) (see Fig. 1). Further details on the principle of operation can be found in the work of Sirota and Wu [23] or in Perino-Gallice et al. [24]. In order to check the reliability of the chamber, a preliminary diffraction experiment was performed with standard DMPC samples, which yielded results (unpublished data) in agreement with literature [25].

The diffraction data were collected on the small momentum transfer diffractometer D16 at ILL [26]. The configuration was optimised to use a 4.75 Å wavelength with a 1% spread. The beam was focussed at the sample position using a pyrolitic graphite monochromator. The sample-detector distance was fixed at 1 m. The goniometer was sealed inside the humidity chamber, and the water reservoirs were filled with heavy

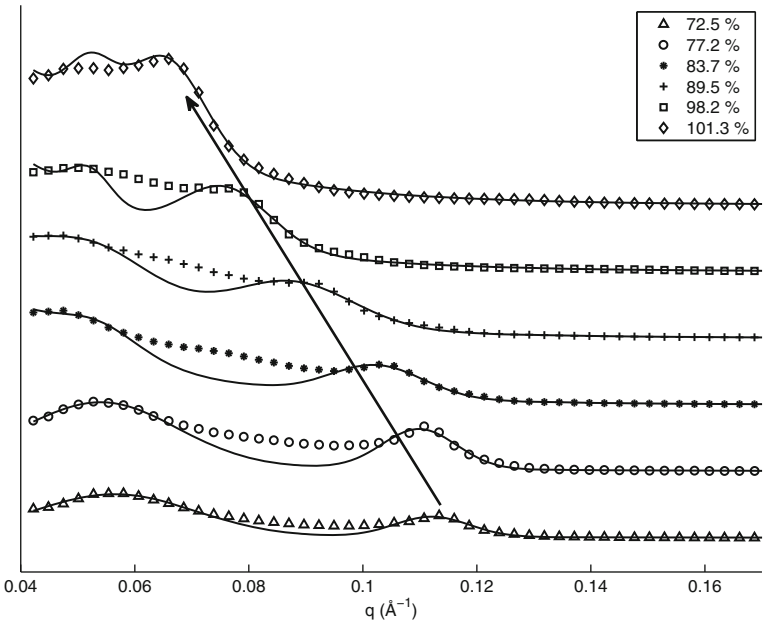

Fig. 2. Data from ϑ scan and their fitted lines are shown for the natural lipid extract; data were collected at 30 °C and at RH ranging from about 72% to about 100%. On the x-axis the momentum transfer q (Å^{-1}) is reported and on the y-axis data are shifted for clarity. The peak at low q increases in intensity as function of RH but it does not change position. The other peak has a shift to lower q with the increase of the relative humidity.

water. The 2-dimensional detector covering a region of 9° allowed ϑ scans (where ϑ is the sample angle) at a fixed detector position of 8 degrees.

3 Results and discussion

In order to study the d-spacing behaviour as a function of relative humidity, measurements were carried out at a fixed sample temperature whilst slowly changing the water reservoir temperature. All samples were measured at 30 °C, because POPE has a phase transition at 25 °C and we were not interested in this transition, but in an equilibrium state. Each other set of measurements (POPG and POPE-POPG-CL) were recorded at room temperature, where possible, in order to reach the maximum value of relative humidity, by reducing the temperature gradient due to the influence of the external environment on the chamber. On the natural lipid sample a set of acquisition was performed at 30 °C. On the POPE sample the three sets of acquisitions were collected at 30 °C. On the POPG sample two sets of acquisitions, at 30 °C and at 27 °C were collected. On the POPE-POPG-CL sample there are two sets of acquisitions, at 30 °C and at 27 °C.

In order to find peak positions ϑ-2ϑ scans were run, then, once the peak positions were found, ϑ rocking curves around these positions were recorded for each water temperature.

Having a 2D detector the raw data were treated with LAMP [27] to obtain a 1D plot. The 1D data were calculated by integrating concentric half rings properly centered. Figure 2 and 3 show examples of the recorded data. Figure 2 shows from ϑ scans the data and fitted lines from the natural lipids collected at 30 °C and at

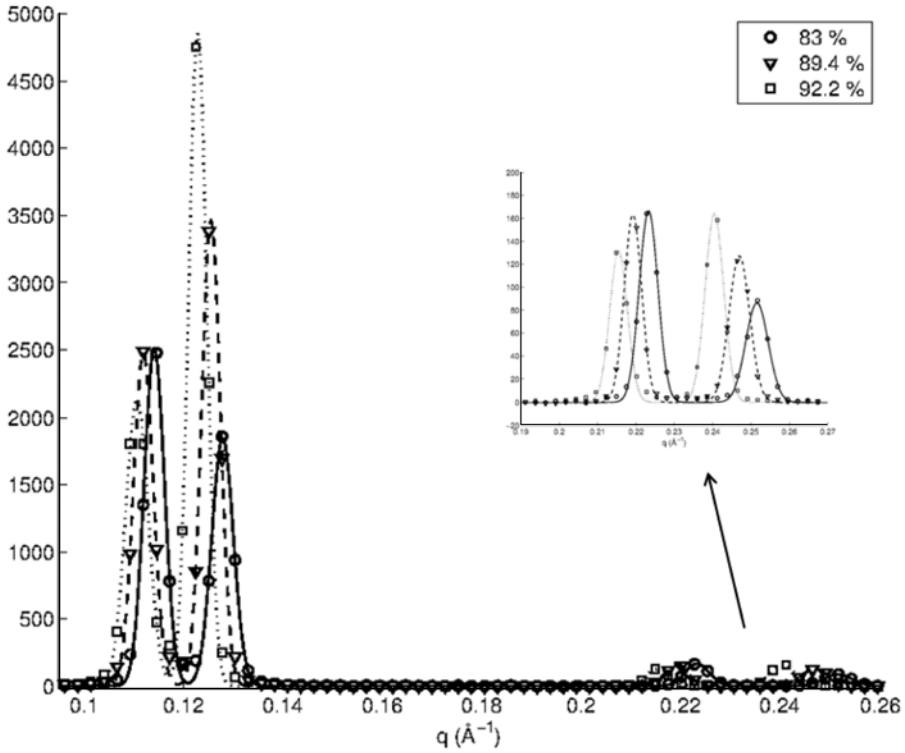

Fig. 3. Data from ϑ scan and their fitted lines are shown for the synthetic mixture containing POPE-POPG-CL at 30 °C and RH ranging from 83% to 92%. On the x-axis the angle q (Å) is reported and on the y-axis data are shifted for clarity. Both peaks move to lower q with the increase of relative humidity.

relative humidities ranging from about 72% to about 100%. Figure 3 shows ϑ scans for the first and second order diffraction peak from the synthetic mixture containing POPE-POPG-CL at 30 °C and relative humidities from 83% to 92%. The momentum transfer values, q (Å^{-1}), is on x-axis and intensity, in arbitrary units, is on the y-axis. For the natural lipid extract data (Fig. 2), again on the x-axis the momentum transfer value is reported.

We obtained two orders of Bragg peaks for the synthetic samples and only the first order for the natural lipid sample. Because of the lower intensity of the second order peaks we show them in different scales of intensity. The experimental data are shown with their best fit to the peak position as a solid line. The fitting procedure was performed by a custom-made program, the background was considered as a decreasing exponential and the peak positions were fitted by a sum of Gaussian function. A generic fitting function is:

$$f(x) = a_0 + b_0 \cdot e^{f\cdot(x-c_0)} + \sum_{k=1}^{n} a_k \cdot e^{-\left(\frac{x-b_k}{c_k}\right)^2}. \quad (2)$$

The coefficients b_k and c_k are given in Å^{-1}, f is given in Å and all the remaining parameters are in arbitrary units.

The *d*-spacing for the natural lipids was calculated with the position of the first order peak on the q-axis by using the formula $d = 2\pi/b_1$. Two first

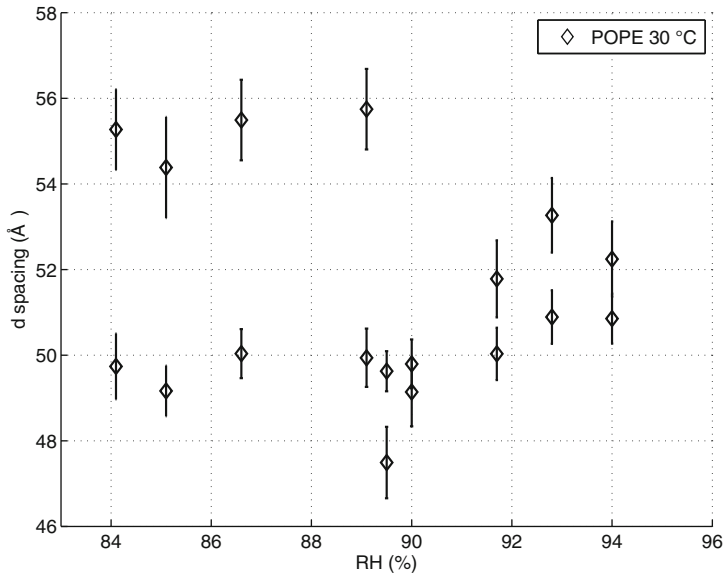

Fig. 4. *d*-spacing as function of RH is shown for the sample of pure POPE, the change occurring around 89% RH can be thought as a phase transition.

order peaks were found in the natural lipids, the one at low q is almost constant over all the relative humidity range, and the other one shifts to higher q with increasing relative humidity as shown in Fig. 2. The two peaks give two different *d*-spacings which are reported in Fig. 6. The error on the *d*-spacing is calculated using c_1, $\Delta d = d \cdot ((c_1/\sqrt[2]{2N})/b_1)$ where N is the number of points used in the Gaussian fit.

For the synthetic lipid samples we had two orders of diffraction and we have used them to calculate the *d*-spacing with the formula $d = 2\pi/(q_2 - q_1)$, where q_1 and q_2 are the positions of the first and second order peak. In the case of the pure POPE sample (see Fig. 4), one of the two phases disappears with the increase of RH. The evolution of the phases over the probed RH range was measured. The two phases are well separated up to 89% RH, and then they seem to move closer to each other. This behaviour can be due to a very slow equilibration of the sample, or else it can be related to a phase transition in correspondence of the relative humidity 89%. It is known that at low humidity content POPE forms hexagonal phases [28].

The pure POPG sample shows a remarkable shift of the peak position, which gives over 94% RH a drastic increase in the lamellar spacing due to electrostatic repulsion (Fig. 5(a)). The sample containing the mixture is characterised by phase coexistence, in fact Fig. 3 shows well separated peaks over all the investigated RH range. The two *d*-spacings increase similarly as function of RH (Fig. 5(b)), it implies the coexistence of two different structures in the sample, very likely different domains as suggested for the natural membrane of *B. subtilis* [5,7].

It was not possible to study the model systems at higher humidity content because of some limitations due to the design of the humidity cell, as it proved difficult to reach high humidities when the gradient with the external temperature is more than a few degrees. Samples were measured at temperatures above 25 °C, the melting transition temperature of POPE, and 100% relative humidity could not be attained. It should be noted that the natural lipid measurements were taken at a different time and with a different chamber not presenting this problem.

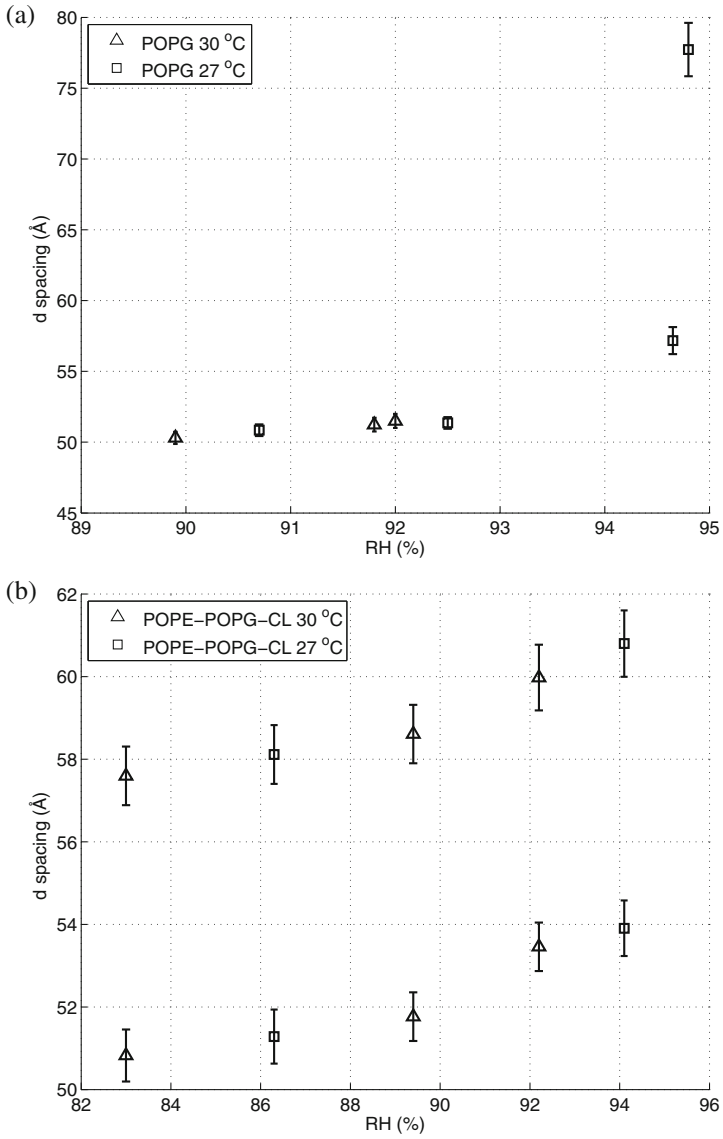

Fig. 5. An overlap of d-spacings trends for two different temperature (30 °C and 27 °C) is shown for POPG (a) and for the mixed sample (b). In both cases the increase as function of RH is not related to the temperature.

4 Conclusion

Neutron diffraction measurements as a function of relative humidity were performed on both natural membranes extracted from *Bacillus subtilis* and synthetic model bilayers with a similar composition to the natural system. The natural system shows the presence of a diffraction peak corresponding to a repeat distance of about 110 Å insensitive to hydration and of a second peak varying with hydration (Fig. 6). The second peak may be attributed to the lipid bilayer matrix of the membrane while the interpretation of the first peak is more challenging. While its position is nearly invariant with humidity content, the intensity increases as the content of water in

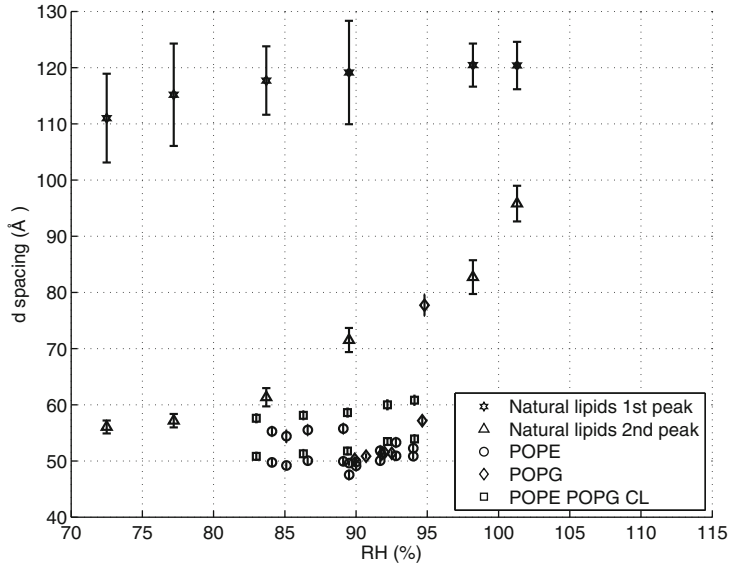

Fig. 6. The lamellar spacings for the natural lipid extract and for the three different synthetic samples are shown. Stars represent the *d*-spacing coming from the natural lipid extract at low q, the triangles represent the *d*-spacing calculated from the other peak. For the model systems (POPE, POPG, POPE-POPG-CL), the *d*-spacings are always under the natural lipid ones, a part from the last point for the POPG sample (diamond), that fits extremely well with the natural lipid *d*-spacing increase.

the system increases (i.e. with relative humidities going from ∼70% to ∼100%). One possibility is the presence of membrane proteins forming a repeat structure in the system only slightly sensitive to hydration. In order to have such a strong signal a non negligible amount of proteins should be present. Although the membrane lipids were purified before use after extraction with non-polar solvents, we cannot exclude that some membrane soluble proteins were not eliminated and remained present in the solvent extraction. Another possibility invokes the presence of a coexistence of lamellar and hexagonal phases in the stack or of line defects as discussed in Rappolt et al. [29].

In the final analysis it seems prudent to attribute the hydration insensitive *B. subtilis* extract peak to the presence of some protein contamination. The hydration-responsive swelling observed in the second peak is consistent with that of a lipid bilayer which contains charged lipid headgroups. According to ref. [12] where Pozo Navas et al. who did small angle solution x-ray scattering on multi-lamellar vesicles composed of various POPG/POPE mixtures, as little as ∼10% PG in the mixture is enough to increase the *d*-spacing from around 60 Å for POPE alone, to about 110 Å and around ∼20% is enough to increase the *d*-spacing to ∼120 Å. They attribute this large *d*-spacing to electrostatic repulsion between the headgroups, since they have no evidence for an increase in bilayer thickness. Given that according to the TLC analysis of the *B. subtilis* lipid extracts, the anionic lipids will be by far in excess, one might expect the extracted lipid mixture to exhibit repeat spacings equivalent to those observed by Pozo Navas et al. [12]. However, if we consider the second peak to represent lamellae formed from a homogeneous mix of the four lipids present in the extract, the influence of the cationic lysyl-PG is likely to dampen the effect of the negative charge and therefore limit the extent of bilayer swelling.

The synthetic lipid data is more difficult to interpret, since one would expect d-spacings comparable with those found for the natural lipids, because there is a similar

excess of anionic lipid, however it should be noted that the relative humidities at which the measurements were taken do not exceed 95%. Thus the maximal swelling of these bilayers will not have been achieved. The presence of two separate phases in the ternary mixture is evident, and may be due to phase separation based on lipid packing geometry as suggested by Domènech et al. [30]. The pure PG lamellae start to swell at the higher RH, to spacings wider than would be expected for neutral lamellar phases (∼60 Å) [12], which indicates that there is an emerging effect of charge repulsion. The phase separation observed in the case of synthetic lipids provides evidence that the phase separation of lipids in the bacterium is to some extent driven by lipid-lipid interactions.

The work presented here grew from a collaboration between Richard Harvey (Pharmaceutical Biophysics Group, KCL) and Giovanna Fragneto (ILL), due to their mutual interest in structural studies on bacterial membranes. The neutron diffraction sample preparation and data analyses were performed by Federica Sebastiani during her time as a visiting student at ILL (supervised by GF) whilst studying for her Masters degree at the University of Rome "Tor Vergata" (Italy). FS is currently a Ph.D. student at the University of Reading (UK) and at the Institute Laue Langevin. The bacterial lipid extracts were prepared by Sarah Khanniche (PhD student at CEA, DAM, Le Ripault) in the D-Lab at ILL, under the supervision of Jean-Baptiste Artero and Michael Haertlein. The authors wish to thank the ILL for awarding beam-time, use of the D-Lab and Soft Matter Laboratory and providing financial support for a training of FS within the PSCM initiative. They also gratefully acknowledge Maikel Rheinstädter and Leide Cavalcanti for their input in the humidity chamber design and commissioning. FS is grateful to Alessandra Filabozzi for useful discussions. RH is financially supported by EPSRC grant EPG0685691.

References

1. C.R. Lammers, et al., Microbiology-Sgm **156**, 849 (2010)
2. Y.M. Zhang, C.O. Rock, Nat. Rev. Microbiol. **6**, 222 (2008)
3. K. Muchova, et al., Res. Microbiol. **161**, 783 (2010)
4. H. Roy, Iubmb Life **61**, 940 (2009)
5. S. Vanounou, et al., Molec. Microbiol. **49**, 1067 (2003)
6. A.B. Hachmann, et al., Antimicrob. Agents Chemotherapy **55**, 4326 (2011)
7. M.H. Foss, et al., Biochemistry **50**, 7719 (2011)
8. I. Barak, et al., Molec. Microbiol. **68**, 1315 (2008)
9. P. Staubitz, A. Peschel, Microbiology-Sgm **148**, 3331 (2002)
10. K.A. Dill, D. Stigter, Biochemistry **27**, 3446 (1988)
11. K.C. Huang, et al., Plos Computat. Biol. **2**, 1357 (2006)
12. B. Pozo Navas, et al., Biochim. Biophys. Acta (BBA) - Biomembr. **1716**, 40 (2005)
13. D.H. Mengistu, et al., Biophys. Chem. **150**, 112 (2010)
14. S. Danner, et al., Biophys. J. **94**, 2150 (2008)
15. E.G. Bligh, W.J. Dyer, Canad. J. Biochem. Physiol. **37**, 911 (1959)
16. J.A. den Kamp, et al., J. Bacteriol. **99**, 298 (1969)
17. K.J. Seu, et al., Biophys. J. **92**, 2445 (2007)
18. J. Vig, J. LeBus, PArts, Hybrids Packaging **12**, 365 (1976)
19. D.G. Bishop, et al., Eur. J. Biochem. **2**, 448 (1967)
20. J. Katsaras, Biophys. J. **75**, 2157 (1998)
21. J. Katsaras, M.J. Watson, Rev. Scient. Instr. **71**, 1737 (2000)
22. A.M. Lanfredi Manotti, A. Tiripicchio, *Fondamenti di chimica* (Casa Editrice Ambrosiana, 2006), p. 656
23. E.B. Sirota, X.Z. Wu, J. Chem. Phys. **105**, 7763 (1996)
24. L. Perino-Gallice, et al., Eur. Phys. J. E **8**, 275 (2002)
25. T.A. Harroun, et al., Phys. Rev. E **70**, 062902 (2004)

26. E. Del Favero, et al., Langmuir **25**, 4190 (2008)
27. LAMP, the Large Array Manipulation Program, `http://www.ill.fr/data_treat/lamp/lamp.html`
28. J. Katsaras, et al., Biochemistry **32**, 10700 (1993)
29. M. Rappolt, et al., Biophys. J. **84**, 3111 (2003)
30. Ò. Domènech, et al., Biochim. Biophys. Acta (BBA) - Biomembr. **1768**, 100 (2007)